Arch. Metall. Mater. **69** (2024), 3, 865-879

DOI: https://doi.org/10.24425/amm.2024.150907

M. YADAV[1], J.K. SAHA[2], S.K. GHOSH[1*]

EVALUATION OF CORROSION BEHAVIOUR OF GALVANISED, GALVALUME AND COLOUR-COATED STEEL SHEETS

In the present study corrosion behaviour of three coated steel sheets in different corrosive environments was evaluated using various characterisation techniques. Multiple types of corrosion tests, like salt spray test, 100% relative humidity test and chemical resistance test, were performed to report the corrosion resistance of samples in different corrosive environments. Enhanced corrosion resistance properties of the colour-coated samples were obtained from all the studies, followed by galvalume and galvanised samples. Cyclic voltammetry reveals a slightly higher pitting for the galvalume sample. SEM, EDS, XRD and Raman analyses for the salt spray tested and 100% humidity tested galvanised samples shows various corrosion products with their morphologies. XRD analysis reveals $Zn_5(OH)_8Cl_2H_2O$ (simonkolleite), ZnO (zinc oxide), β-Zn $(OH)_2$, Zn $(OH)_2$ (zinc hydroxide) and Zn $(ClO_4)_2$ for salt spray tested samples whereas for the 100% relative humidity tested samples, main corrosion products are ZnO (zinc oxide), β-Zn $(OH)_2$, Zn $(OH)_2$ (zinc hydroxide), Fe and Zn. Raman spectroscopy reveals the presence of ZnO, β-FeOOH, white rust, green rust, $FeCl_2$, Fe_3O_4, FeOH, Fe_2O_3 and δ-FeOH for salt spray tested samples, but for 100% humidity test, only ZnO is revealed.

Keywords: Galvanised; Galvalume; Colour-coated steel; Corrosion; SEM; X-ray diffraction

1. Introduction

The use of precoated steel is dominant in industries and other sectors mainly due to the economic benefits and lower environment-polluting effects [1-3]. A higher resistance to corrosion is required for these steels because corrosion degrades the structures and reduces their strengths with different levels of impact, starting from human safety concerns to resource and environmental degradability. The zinc-rich galvanised coatings are mostly used for anti-corrosion resistance. Hot dip galvanising steel sheet is used in the automotive, building and household appliance industry, and construction sector due to its excellent resistance to corrosion, durability, low maintenance, economic benefits, and low environmental impact [1,2,4-7]. However, in industrial and severe marine environments, zinc coating fails due to the highest dissolution rate of zinc [8]. To overcome this limitation, an aluminium coating can replace zinc coating, but they have weak cathodic protection effects, and thereby, Zn-Al coatings are developed [8]. Corrosion resistance can be improved further by adding various alloying elements of Al, Mg, Co, Ni, and Mn to this coating system [4,6]. The use of Zn-Al coatings in galvalume (Zn + 55 wt.% Al + 1.6 wt.% Si) steels with higher aluminium are better for higher corrosion resistance [9-12]. Although a better performance of these steels over the conventional galvanised steel in marine and industrial environments due to sacrificial anodic protection of zinc and aluminium oxide barrier properties was reported earlier, the results show some scatters based on their performances for the application areas such as acidic, industrial, marine, household chemicals, atmospheric and other environments and these collective results are also rarely found in the literature [11-12]. In addition, aluminium also supports the formation of a thin $Fe_2Al_5/FeAl_3$ layer on the interface of coating/steel, which reduces fragile and brittle Fe-Zn intermetallic formation to improve the coating adhesion with the substrate and suppresses the formation of dross [1]. The use of silicon as an alloying element to control the intermetallic layer thickness, which forms at the interface, along with its ability to control the exothermic reaction between the metal and the steel substrate, is well known [8-9]. From an application point of view, galvalume steel is used widely in the electric motor housing, door plate, window drive rails, electronics boxes, roof air-conditioner equipment, appliances, automotive underbody parts and high-temperature applications [12]. The use of polyurethane coating as corrosion protection is reported in the literature [1,13-14]. These

[1] DEPARTMENT OF METALLURGY AND MATERIALS ENGINEERING, INDIAN INSTITUTE OF ENGINEERING SCIENCE AND TECHNOLOGY, SHIBPUR, HOWRAH -711103, INDIA
[2] S J ENGINEERS & CONSULTANTS, 35D, CHARU AVENUE, KOLKATA – 700033, INDIA

* Corresponding author:skghosh@metal.iiests.ac.in

types of steel are widely used in the construction of buildings and bridges [14]. Painting or colour coating protects the steel from harsh corrosive environments due to its barrier properties.

Metallic corrosion ability depends on the characteristics of the metal surface, a protective interphase film formed by metal, the protective films' physical, electrical, electrochemical properties and the external environmental exposure conditions for the system. The corrosion resistance ability of zinc comes from its barrier property, via which it corrodes before bare metal and galvanic protection, due to which sacrificial anodic protection occurs [15]. For galvalume steel, the lesser solubility product of hydroxide of aluminium (1.3×10^{-33} M at 25°C) compared to zinc (3×10^{-17} M at 25°C) allows the formation of Al_2O_3 passive layer compared to pure zinc coatings [16-17]. For colour-coated steel, better coating properties of polyurethane provide good corrosion resistance.

Various studies were performed earlier on the galvanised, galvalume and other types of coatings along with their corrosion resistance behaviour. Arianpouya et al. have reported that polyurethane/zinc/nanoclay additions to zinc-rich coatings enhance the resistance to corrosion [1]. They have reported that in the coatings, nanozinc and nanoclay can act as barrier pigments to improve the resistance to corrosion for zinc coatings. In another study, Schuerz et al. developed a Zn-Al-Mg coating and reported its superior corrosion resistance due to forming a stable adherent Al_2O_3 oxide layer [4,11]. While Zhang et al. have performed a study on galvalume steels to understand their corrosion behaviour in rainwater, chloride-containing environments and simulated automotive environments and reported enhanced performance due to the Al_2O_3 passive layer along with the effect of zinc release rate and its impact on corrosion behaviour [12,18]. Manna et al. have reported better corrosion performance due to higher Al addition in Zn-Al coating [19]. Li et al. have identified the effect of superhydrophobic coatings on galvanised steel for better corrosion resistance and self-cleaning property [20]. In another study, Sergienko et al. studied the effect of superhydrophobic phosphate-siloxane film on the improved corrosion performance of galvanised steel in corrosive atmospheres of high humidity and salt spray [21]. In various kinds of literature, corrosion behaviour with their mechanisms for coated steels is discussed [16,22]. However, the research hunt for finding strong, adhesive, and highly corrosion-resistant coating for the protection of steel continues.

The current research is performed to study the corrosion behaviour of galvanised, galvalume and colour-coated steels. The comparative study among all three coated samples will provide research findings on corrosion tests on different application areas such as salt spray for marine, humidity test for moisture, chemical resistance test for household application, and cyclic voltammetry for the industrial environments to choose the application-specific materials. The experimental results can be reliably used for selecting the suitable material based on the environmental condition, expected life and cost parameters (one-time cost and life cycle cost). Furthermore, the combined results of the chemical resistance tests are not reported, which is a new addition to our study. The corroded surfaces and corrosion products are characterised and analysed. Finally, a comparison has been made to thoroughly understand the corrosion performance of three steel sheets in various corrosive environments and their corrosion mechanisms.

2. Experimental procedure

2.1. Materials

The current study was performed on three types of steel sheets, i.e., galvanised, galvalume and colour-coated steel sheets. The sheet coils were produced by hot rolling, followed by degassing, pickling, fluxing and cold rolling processes. Samples for the present study were received in sheet form from JSW Steel Coated Products Ltd., Vasind Works, Maharashtra, India. An optical emission spectrometer (Thermo 3460) was used to analyse the chemical composition of all three samples, as shown in TABLE 1.

TABLE 1 depicts the composition of the substrate made of low carbon steel. Almost similar composition for these steels was evident from TABLE 1, with a lesser amount of carbon and small Al addition for deoxidation purposes. The designation of the kind of steel used in the present study was IS 2062:2011 (ISO 630-2:2021, Structural steels-Part 2: Technical delivery conditions for structural steels for general purposes). The steel substrate contains carbon only from 0.04% to 0.05% and hence they are easier to cold form, making them easier to handle and convert to malleable and ductile products easily. For the galvanised steel sample, the coating was pure zinc, whereas the galvalume sample consisted of Zn-Al alloy coating having 55% Al, 43.4% Zn and 1.6% Si and the colour coating was made of polyurethane coating on the galvanised substrate. For the colour-coated steels, the substrate was given the final paint coating for additional protection to withstand harsh weather conditions and longer life. Colour coating was continuously applied to the surface of the steel substrate.

TABLE 2 depicts the details of the type, weight, and thickness of the applied coating on the surface of the steel substrate.

TABLE 1

Chemical composition (wt.%) of the low carbon steel substrate

Type of steel sheet	C	Mn	P	S	Si	Al	Fe
Galvanised	0.052±0.001	0.106±0.020	0.009±0.002	0.005±0.001	0.014±0.001	0.037±0.001	Balance
Galvalume	0.041±0.002	0.112±0.013	0.008±0.001	0.005±0.001	0.015±0.002	0.055±0.001	Balance
Colour-coated	0.041±0.003	0.112±0.024	0.007±0.002	0.004±0.001	0.015±0.002	0.040±0.001	Balance

The coating weight for galvanised and galvalume samples was 275 g/m^2 and 150 gm/m^2, respectively and no top coating was applied on their surface, whereas for colour-coated samples, polyurethane coating of 124 g/m^2 was applied over the surface of Zn primer coating.

TABLE 2

Details of the coating

Sample	Sample code	Primer	Top coat	Weight (g/m^2)	Thickness (μm)
Galvanised	GI	Zn	Uncoated	275	51.38
Galvalume	GL	Zn-Al	Uncoated	150	54.40
Colour-coated	CC	Zn	Polyure-thane	124	25.10

2.2. Corrosion testing methods

Accelerated corrosion tests were performed to find the corrosion resistance of all the experimental samples. The corrosion behaviour and white rust resistance studies against atmospheric exposure conditions were performed on the pieces of 6-inch × 3-inch size. Traditional neutral salt spray (NSS) test conforming to ASTM B117 standard was used for this purpose which is widely used to study corrosion protection of protective coatings [1,5,23]. For this test, 5% dilute NaCl solution was prepared to analyse the test sample exposed for 600 h. The temperature of the salt spray chamber was maintained at 35°C and the pH of the solution was regulated at 6.7 throughout the test according to the standards of ASTM B117. The average collection rate for a horizontal collecting area of 80 cm^2, according to ISO 9227:2017-06, was 1.5 ml/h. Extended uncertainty of the determined parameters was estimated for a confidence level of 95% in the NSS test. The edges of all the samples were protected during the test by sealing them with high-build epoxy paint and the images were collected from the exposed portion in a salt spray test. A 100% relative humidity test conforming to the ASTM D2247 standard was performed to analyse the rate of corrosion for all the experimental samples. 100% relative humidity was chosen to mimic the rainfall environmental conditions. For this study, samples were placed in a heated and fully saturated air and water vapour mixture where the 100°F(38°C) temperature was maintained in the chamber. To ensure the effective resistance of coatings against the household chemicals, the chemical resistance test conforming to ASTM D1308 standard was performed. For this test, 30% H_2SO_4 solution was used at a pH of –0.99 and the test was performed for 24 h, whereas for the alkali test, 20% KOH solution at a pH of 14.6 and for solvent acetone solution at a pH of 7 was used and tested for 24 h.

Cyclic voltammetry was also performed in order to understand the pitting corrosion behaviour of the samples in HCl solution. A working electrode of embedded specimens, a counter electrode (Pt-Rh mesh) which was placed to one side of the samples and an independent reference electrode of glass-lined saturated calomel (SCE) were used to perform the electrochemical measurement. The study was performed in Origalys Potentiostat, combined with Origamaster 5 module. For this study, samples were cut into a size of 10 mm × 10 mm and a standard solution of 1% HCl solution was chosen to mimic the acid rain and industrial environment. The potential scanning rate used for the sample was 1mV/sec and scanning range used was –1 to +1 Volts and the current range used in the test was –100 to +100 mA.

2.3. Characterisation

For microstructural characterisation for all the samples, scratch-free surfaces were prepared via standard metallographic techniques like grinding (belt and paper), cloth polishing (coarse and fine) and etching with 5% Nital solution. For observing the microstructural constituents, an inverted optical microscope (Carl Zeiss Axiovert 40 Mat) was used. In order to study the corrosion product morphology of all the samples corroded via salt spray, 100% humidity and cyclic voltammetry test, SEM (HITACHI, S-3400N) was used at an operating voltage of 15 kV in secondary electron imaging mode. Energy dispersive spectroscopy (EDS) analysis was performed for the chemical analysis of all the corroded samples and for that purpose, surface sputtering was done using a gold ion beam (HITACHI E-1010 ion sputter) to avoid charging and obtaining high-quality images [24-25]. Samples were characterised further via the 'Bruker-advance D8' XRD machine integrated with a copper (CuKα) target and operated at 40 kV voltage and 30 mA current [25]. The dimension of the sample used for this study was 15 mm × 15 mm. XRD data were collected over a range of 2θ values from 10-90° with a step of 0.01s^{-1}. The measured diffraction patterns were analysed further using the Profile Fit Software Metal Jet and Turbo X-ray source. Phase identification was made further by matching the experimental data with JCPDS files using X'Pert High Score Plus software. Raman spectroscopy was conducted further to confirm the corrosion product/compound formed on the sample surfaces of the galvanised sample after salt spray and 100% humidity tests.

3. Results and discussion

3.1. Corrosion behaviour

3.1.1. Salt spray test

Fig. 1 depicts the appearance of all the salt spray-tested steel sheet samples. The galvanised steel sample (Fig. 1a) underwent higher corrosion than the other two. The formation of red and white rust over the galvanised steel surface during a salt spray test is a common phenomenon reported earlier [2,11,26-29]. The appearance of the initial white layer is due to the formation of ZnO, which after severe corrosion, degrades to form red rust on the metal surface due to corrosion of underlying low carbon steel. Besides, the white rust layers show poor adherence to the

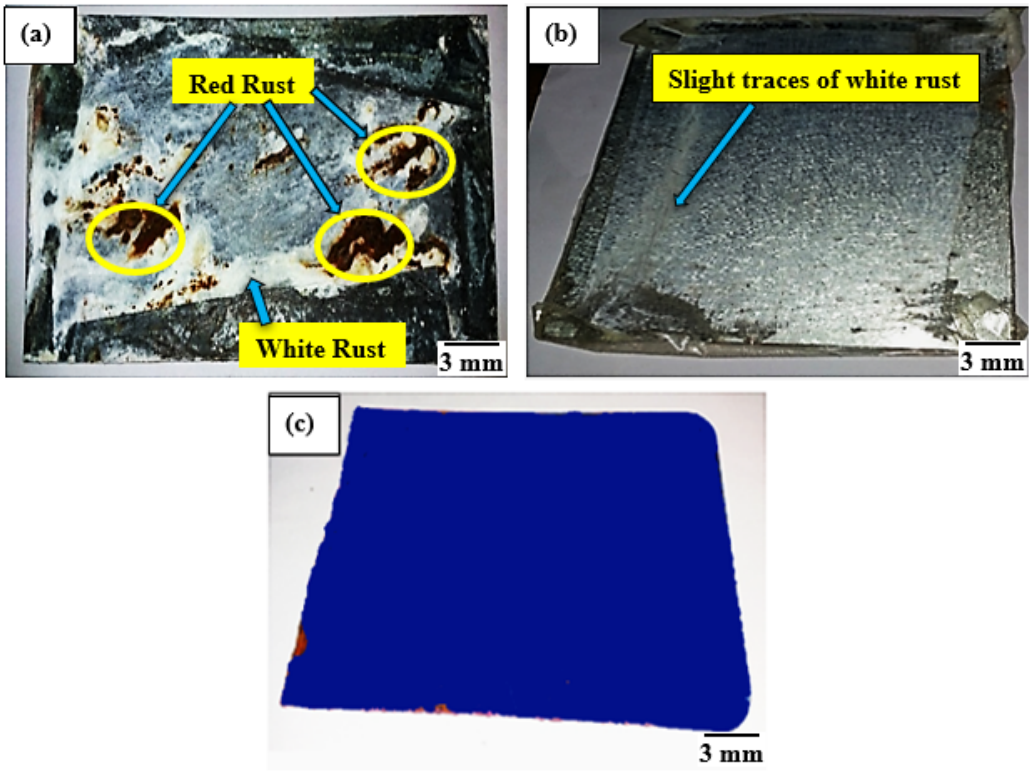

Fig. 1. The appearance of samples after salt spray test for (a) galvanised, (b) galvalume and (c) colour-coated steel sheet

metal surface; thereby enhancing corrosion. For the galvalume sample, slight traces of white rust formed and even after 600 h, no red rust is evident due to the presence of aluminium in the coating. The higher corrosion resistance of galvalume steel compared to galvanised steel in salt spray test has been reported earlier [4,8,10-11,28,30-31]. This is because the zinc coating is unable to resist the corrosion of the galvanised steel. Chloride ions degrade the coating by acting as a chemical degradation factor [10,32]. This coating of ZnO breaks via its reaction with the salt, which acts as a corrosive media for the sample; thereby exposing the bare steel surface through which corrosive salts can easily pass to cause the corrosion and these corrosive products appear in the brownish-red colour distributed heterogeneously over the sample surface. But for the galvalume sample, the presence of the higher amount of aluminium in the substrate (0.055 wt.%) (Fig. 1b vis-à-vis TABLE 1) and in the coating provides a higher corrosion resistance as aluminium provides a well adherent, dense Al_2O_3 oxide layer over the metal surface which stops the corrosives from entering the surface of the metal [4,8,11,16,33]. So, the key reaction is the conversion of Zn-Al coating into an Al_2O_3-rich oxide layer which enhances the corrosion resistance of the galvalume specimen. It is known that a better coating adhesion and its homogeneous distribution over the metal surface provide enhanced resistance against corrosion. Zn-Al metallic coatings for galvalume sample offers 3-6 times better coating resistance compared to Zn coatings which were reported earlier [10,16]. The lower coating resistance can start the substrate corrosion, which was supported by corrosion product development which reduces the coatings barrier properties by creating stresses at the interface of the coating and the substrate. Zn-Al alloy coatings decrease this type of substrate degradation; thereby maintaining a higher resistance to corrosion. Some kinds of literature have reported corrosion of galvalume samples even after 1 to 7 days of salt spray test [18]. However, a strong adherent coating does not reveal corrosion even after 25 days (600 h) in the present study, whereas in the previous case, poor coating adhesion with the substrate might have resulted in the reported corrosion behaviour. The surface of the colour-coated steel sheet (Fig. 1c) is free from corrosion mainly due to the strong adherent polyurethane coating, which does not allow the penetration of the corrosive salts to enter the metal surface, thereby preventing the corrosion as reported earlier [1,13]. So, the salt spray test denotes the higher corrosion resistance of colour-coated steel, followed by galvalume and galvanised steel.

3.1.2. 100% Humidity test

The inability to show little differences makes the salt spray test a less precise test and thereby, other tests were also performed on the samples. Fig. 2 depicts the appearance of all the 100% humidity-tested steel sheet samples. The galvanised steel sample (Fig. 2a) again underwent higher corrosion compared to other samples. Furthermore, a higher relative humidity leads to enhanced corrosion because of the presence of a thin water layer over the surface of the sample, which breaks the coating layer of zinc in galvanised sample easily. Besides, water vapours, oxygen and other gases are usually present at the metal-coating interface, which leads to substrate corrosion under certain conditions. The coating of ZnO breaks via moisture which acts as

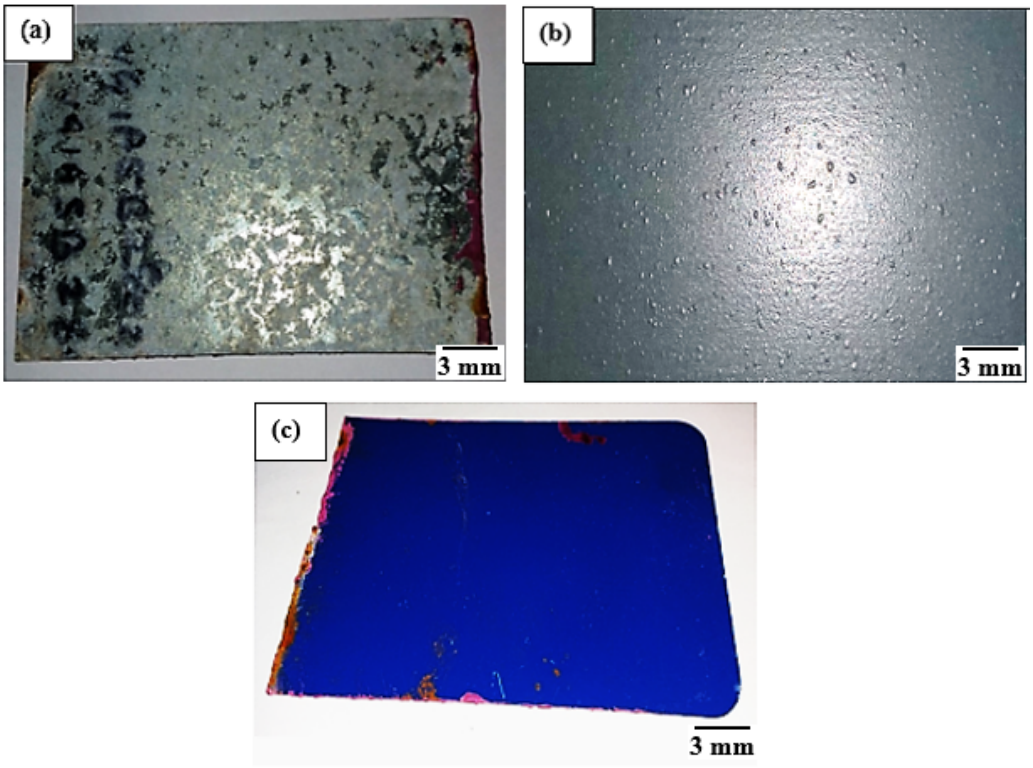

Fig. 2. The appearance of samples after 100% humidity test for (a) galvanised, (b) galvalume and (c) colour-coated steel sheet

a corrosive media and exposes the bare steel sample surface; thereby making an easy pathway for corrosive salts to cause the corrosion. However, the higher aluminium provides higher corrosion resistance to the galvalume steel sample compared to galvanised, as reported earlier, and due to that, only a slight white layer is observed (Fig. 2b) [4,8,10,16,33]. On the other hand, the colour-coated steel sheet (Fig. 2c) is fully corrosion resistant due to strong adherent polyurethane coating and its corrosion resistance property, although some holiday defects were evident in Fig. 2b. Hence, the 100% humidity test is well correlated with the salt spray test and the corrosion behaviour of all three samples follows a similar trend as observed for the salt spray test.

3.1.3. Chemical resistance test

Results of the chemical resistance test are summarised in TABLE 3, which shows that all three samples are corrosion resistant to the acetone solution, which is well expected due to the neutral nature of this solution. But when exposed to the 30% sulphuric acid (H_2SO_4) solution and 20% caustic potash (KOH) alkali solution, it is observed that galvanised sample shows severe corrosion compared to the galvalume sample due to the peeling of zinc coating. In a 20% KOH solution, galvanised steel undergoes severe corrosion via proton reduction with hydrogen evolution which is the main reaction in the alkaline medium [26]. Furthermore, the reaction rate increases with a higher acidic

TABLE 3

Results of chemical resistance tests

Serial No.	Sample	Test Name	Observation
1.	Galvanised Steel	Resistance to 30% sulphuric acid (wt. by volume)	Severe corrosion observed on the panel
		Resistance to 20% caustic potash (wt. by volume)	Severe corrosion observed on the panel
		Resistance to solvent (acetone)	Did not show any sign of blistering, wrinkling & lifting of the film, with no change in colour
2.	Galvalume steel	Resistance to 30% sulphuric acid (wt. by volume)	Panel dissolved in acid solution
		Resistance to 20% caustic potash (wt. by volume)	Severe corrosion observed on the panel
		Resistance to solvent (acetone)	Did not show any sign of blistering, wrinkling & lifting of the film, with no change in colour
3.	Colour-coated steel	Resistance to 30% sulphuric acid (wt. by volume)	Did not show any sign of blistering, wrinkling & lifting of the film, with no change in colour
		Resistance to 20% caustic potash (wt. by volume)	Did not show any sign of blistering, wrinkling & lifting of the film, with no change in colour
		Resistance to solvent (acetone)	Did not show any sign of blistering, wrinkling & lifting of the film, with no change in colour

environment for the galvanised steel, which is well known for H_2SO_4 solution due to enhanced diffusion rate and active species ionization in the corrosion reaction [34]. Accelerated rates of corrosion were obtained for the acidic nature of the solution via enhancing the cathodic reduction of hydrogen ions over the surface of the metal [31]. Aluminium is mainly responsible for lesser corrosion on galvalume steel sheets when compared to galvanised steel sheet. Some amount of corrosion is seen for the galvalume sample in an acidic solution due to the aggressive corrosion behaviour of this solution, but it still shows comparatively higher corrosion resistance than galvanised steel [8]. The colour-coated steel did not undergo any form of corrosion due to the strong adherent polyurethane coating. The colour-coated panels did not show any sign of blistering, wrinkling, and lifting of film, and no change in colour was observed. Hence it depicts superior corrosion resistance among all the samples in the current study [1,13].

3.2. XRD study of corrosion product

After conducting the salt spray and 100% humidity tests, the corrosion products deposited on the surface were examined by XRD analysis. Fig. 3 shows the XRD profiles of the galvanised sample after the salt spray test (Fig. 3a), 100% relative humidity test (Fig. 3b) and uncorroded sample before the corrosion test (Fig. 3c). The galvalume and colour-coated samples are not studied via XRD analysis as they have shown almost no corrosion due to enhanced coating properties to act as a barrier against corrosion. For the salt spray tested sample, the X-ray profile primarily reveals $Zn_5(OH)_8Cl_2H_2O$ (simonkolleite), ZnO (zinc oxide), β-Zn $(OH)_2$, Zn $(OH)_2$ (zinc hydroxide) and Zn $(ClO_4)_2$ which are consistent with those reported earlier [4,6-7,18,22,33,35-37]. For the 100% relative humidity tested sample, the main corrosion products are ZnO (zinc oxide), β-Zn $(OH)_2$, Zn $(OH)_2$ (zinc hydroxide), Fe and Zn which agree with the earlier studies [7,36,38-39]. The appearance of Zn $(OH)_2$ indicates the basis of the formation of other corrosion products for the 100% relative humidity tested sample. The white rust areas on the salt spray tested galvanised sample mostly consist of Zn $(OH)_2$ and $Zn_5(OH)_8Cl_2H_2O$ which are also found in the XRD study and hence both the results are well corroborated. The occurrences of $Zn_5(OH)_8Cl_2H_2O$ and Zn $(OH)_2$ can reduce the oxygen reduction reaction and thereby improve the corrosion resistance initially for galvanised samples and due to that cyclic voltammetry results, a passivation zone for this sample which gets broken again because these corrosion products fail to maintain their continuity throughout the surface of metal due to the formation of loose, porous corrosion products which reveals the bare metal surface for corrosion [2,4,6,40-42]. The initial appearance of white corrosion products is due to the formation of ZnO, which is seen from the visual inspection of both salt spray and 100% humidity-tested samples. The Zn $(ClO_4)_2$ detected by XRD in the presence of NaCl also play an essential

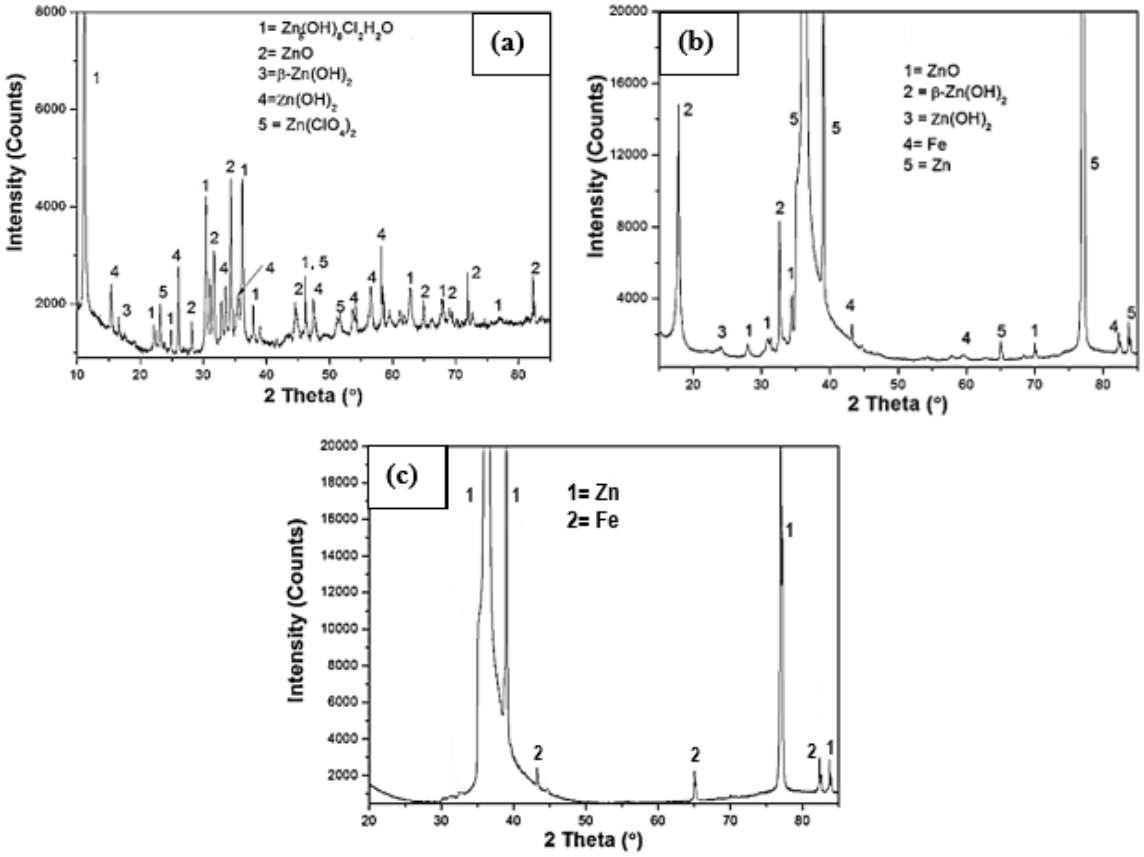

Fig. 3. XRD profiles of (a) salt spray corroded galvanised sample, (b) 100% humidity test corroded galvanised sample and (c) uncorroded galvanised sample

role in continuing corrosion due to the breakdown of the rust layer, as mentioned in a previous study [43]. The uncorroded sample (Fig. 3c) reveals the presence of Fe and Zn, which are well expected for the uncorroded galvanised steel.

3.3. Raman spectroscopy

TABLE 4

Corrosion products with their respective wavenumber peaks

Wavenumber (cm^{-1})	Material compound
103.18	ZnO
310	β-FeOOH (Akageneite)
381	White rust [$3Zn(OH)_2ZnCl_2(OH)_4$]
439	Green rust
565	ZnO (Zinc oxide)
610	$FeCl_2$
668.71	Fe_3O_4 (Magnetite)
688	FeOH
1320	Fe_2O_3 (Haematite)
1340	δ – FeOH (Ferroxyte)

Figs. 4a and 4b show the Raman spectroscopic analyses for salt spray and 100% humidity-tested corroded galvanised samples. TABLE 4 shows the corrosion products with their respective wavenumber peaks. As per the comparison ZnO, β-FeOOH, white rust, green rust, $FeCl_2$, Fe_3O_4, FeOH, Fe_2O_3 and δ-FeOH are present for salt spray tested specimen, whereas only ZnO is present for 100% humidity corroded specimen. Iron oxide and oxyhydroxides are usually observed as mixtures in corrosion films due to their higher structural relationship [44]. Green rusts, commonly known as iron hydroxyl salts, are a member of the divalent-trivalent ionic compounds class and stacked layers of Fe $(OH)_2$, which carries positive charge due to the presence of $Fe^{[III]}$ and inter-layers constituted of anions and water molecules. White rust regions mainly consist of ZnO-rich regions always. The higher iron oxide products resemble the presence of red rust area, which might be analysed with the white rust area as zinc corrosion products form the white rust area, and this study corroborates well with visual analysis of salt spray tested samples. Raman band at 310 cm^{-1} is a characteristic of akageneite and is often seen as a product of corrosion in environments of higher chloride contents where high Fe is found, meaning in red rust areas [36-37]. The appearance of higher red rust for the galvanised sample can be due to akagainite (β-FeOOH) formation as reported earlier [16,35-37]. Furthermore, atmospheric CO_2 dissolves in the surface electrolyte and makes it acidic by forming carbonic acid, and further reaction gives hydrozincite and the formation of zincite and hydrozincite enhanced with an increase in relative humidity [39]. However, zincite (ZnO) is dominantly observed in the Raman analysis because the low CO_2 environment has been used in the test that usually forms only zincite over the metal surface as low CO_2 environments fail to acidify the water to form carbonic acid. So the zincite cannot be converted to hydrozincite [39].

3.4. Cyclic voltammetry

Fig. 5a shows the cyclic voltammetry results of all the experimental samples plotted together. Cyclic voltammetry was performed mainly to determine the pitting corrosion susceptibility of the metal. It has been reported that for the galvalume sample, the most aggressive corrosive environments are acidic environments, as the Zn-Al coating usually has weak protecting properties in these environments, which leads to slightly higher corrosion compared to galvanised steels. The smallest radius and volume make the Cl^- ion strong anodic activator and allow it to penetrate the rust layers and destroy the rust layer to react directly with the metallic substrate. Furthermore, Cl^- ions are hygroscopic in nature which initiates pits on the sample surface by its adsorption on the passive film and leads to localized corrosion to destroy the coating by forming water-soluble compounds [3,7,35,45]. The destruction of the rust layer via Cl^- ion makes the zinc coating to appear as an anode and other entities of the intact rust layer as a cathode which leads to the formation of an activation-inactivation cell where smaller anodic and larger cathodic areas accelerate the pitting corrosion. It is well-established that lower corrosion current values lead to the enhanced corrosion

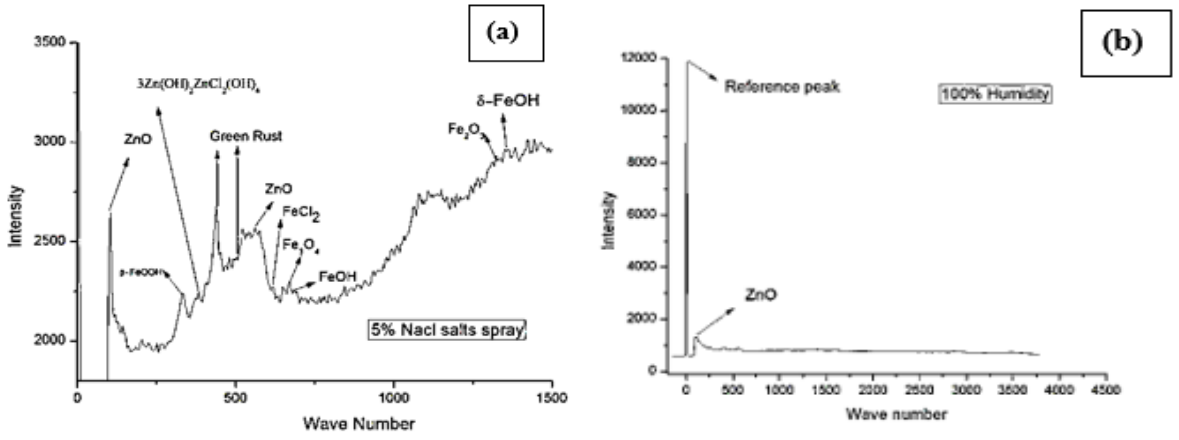

Fig. 4. Raman analysis plot for (a) salt spray tested galvanised sample and (b) 100% humidity tested galvanised sample

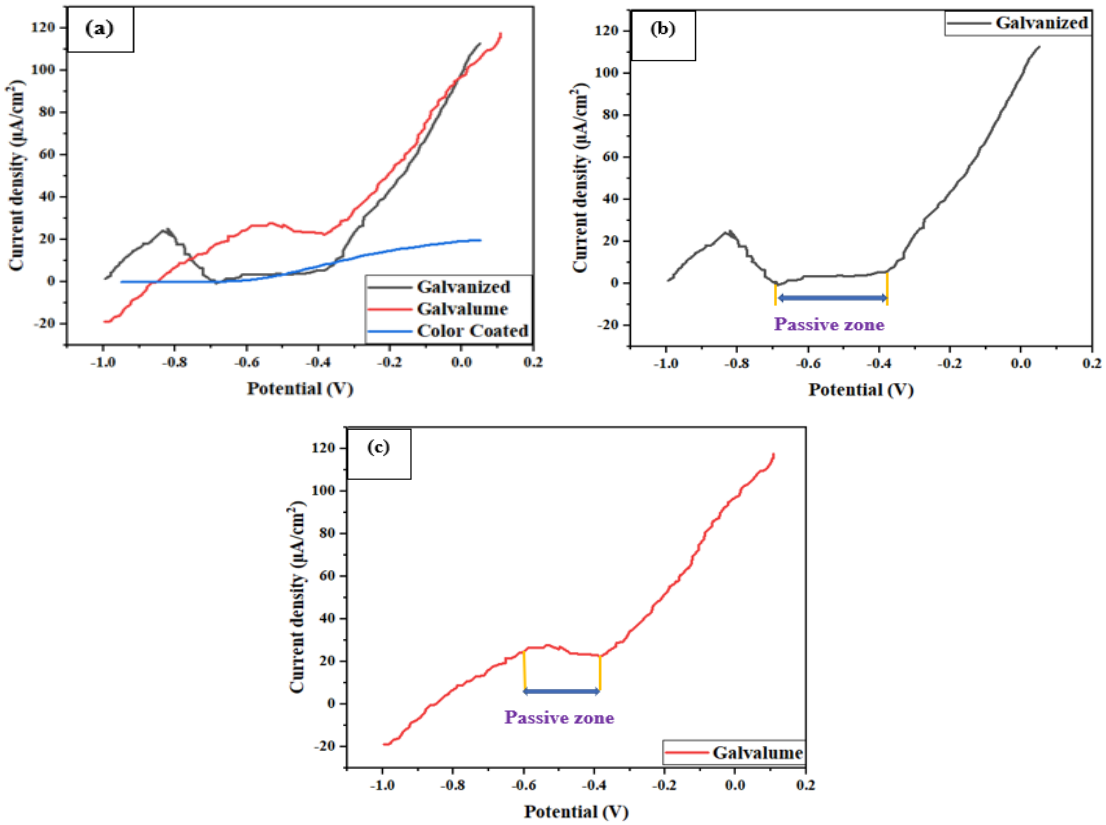

Fig. 5. Cyclic voltammetry results for (a) all experimental samples, (b) galvanised and (c) galvalume steel samples

resistance of the sample [25]. For galvanised steel sample, as seen from Fig. 5b, the corrosion current keeps on increasing with applied potential initially, but the curve dips again with lower corrosion current values and then maintains itself at this place for a certain potential increase due to the formation of the passive layer of simonkolleite $Zn_5(OH)_8Cl_2.H_2O$ which protects the bare metal surface from corrosion initially due to its compact morphology along with the low electron density and layered structure with decreased ion-transfer through the layers. But it fails to maintain uniformity throughout the surface and is present locally. So, the surface of the metal becomes porous, and higher chloride penetration starts again, which dissolves the passive layer and hence corrosion current increases again to show higher corrosion with the rise in potential. The observed plateau is associated with the passivity because the current density decreases with increasing corrosion potential in this region. It is well known that a decrease in the corrosion current and an increase in the corrosion potential always lead to enhanced corrosion resistance. Besides, the rate of decline in the corrosion of galvanised steel with an increase in potential is mainly due to the faster rate of hydrogen evolution in the HCl solution. For galvalume coatings, the anodic polarization curve (Fig. 5c) has a unique shape which resembles the two-stage corrosion process that corresponds to the oxidation of zinc and aluminium. For the galvalume sample, corrosion behaviour increases slowly and then sharply with an increase in potential as the zinc layer starts to corrode, but the presence of aluminium allows the formation of the strong and adherent passive Al_2O_3 layer, which protects the metal surface from corrosion and so a passive region with constant current is evident. After that, the corrosion current increases at a rate like that of galvanised steel with a further increase in the potential. It is noteworthy that a similar trend in the corrosion behaviour of galvanised and galvalume samples has been reported earlier [9,19,45]. The colour-coated sample, due to polyurethane coating, remains almost free from corrosion due to better coating performance, and as a result, the current density increases at an excessively slow rate with an increase in potential which is well below those of the galvanised and galvalume samples [1,13]. So, the enhanced corrosion resistance of colour-coated steel is obtained, followed by galvanised and galvalume steel in acid rain and industrial environments.

3.5. Corrosion micrographs

3.5.1. SEM and EDS analyses after salt spray

Fig. 6 shows the SEM micrographs of corroded galvanised samples at different magnifications (Fig. 6a-c). It is noteworthy that the galvalume and colour-coated samples are not studied via SEM and EDS analyses after the salt spray test as they have shown almost no corrosion on the surface of samples due to enhanced coating properties to act as a barrier against corrosion. The uncorroded region (Fig. 6a) appears compact and smooth without any corrosion product, whereas the corroded area reveals rough/uneven corrosion products. It has been reported earlier that

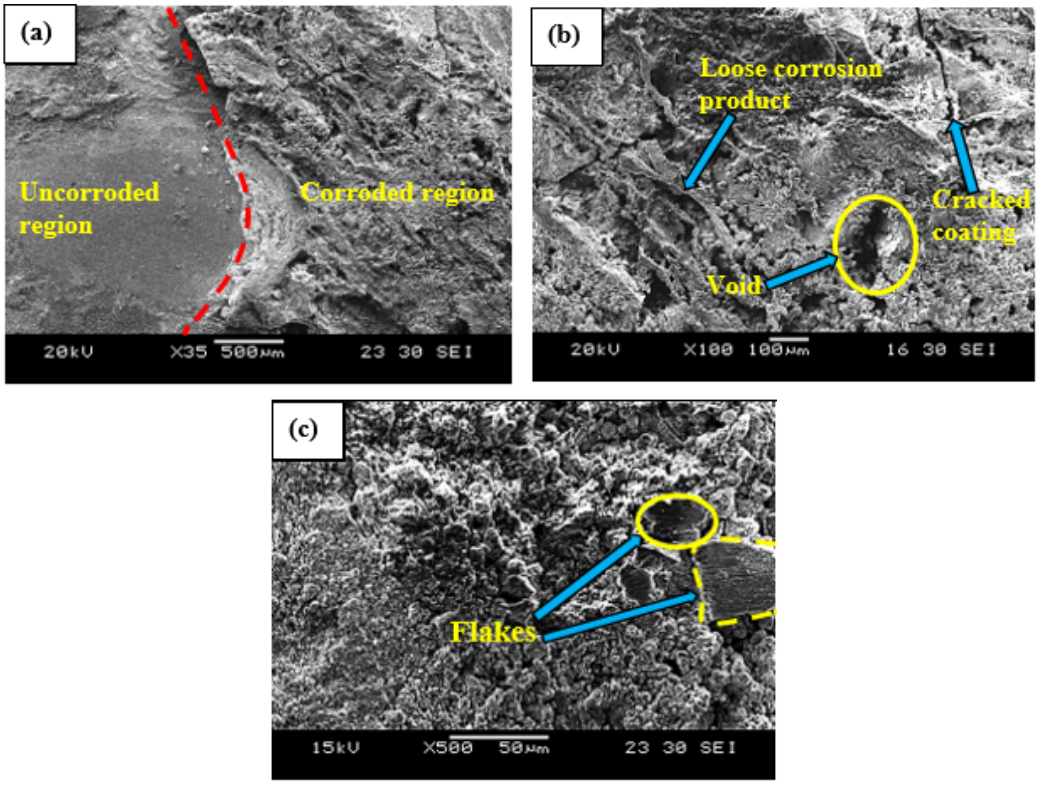

Fig. 6. SEM micrographs of (a) both uncorroded and corroded regions, (b) void, cracking, loose corrosion product and (c) flakes on the galvanised sample

the galvanised steel fails to maintain its passivity in NaCl solution [6]. The presence of NaCl accelerates the corrosion of Zn by absorbing water vapour from humid air; thereby forming thin electrolyte films to enhance the corrosion drastically. With time Cl^- damages the rust layers to create the void, loose corrosion products and causes cracks in the coatings, as seen in Fig. 6b, which might be due to the corrosion creep mechanism [6,10]. The appearance of the crack in the coating is mainly due to poor flexibility and low adhesion of the coating, and consequently, a high white rust formation is seen. Porous zinc corrosion products with many voids along with flakes, as seen in Figs. 6b and 6c, are consistent with earlier studies revealing that zinc coating is not well adherent with the metal surface [11,22]. These flakes resemble the simonkolleite product [29]. Furthermore, cracking and flaking (Fig. 6b to c) in the coating enhance the corrosion rate of the samples. The formation of the porous layer of rust over the metal surface enhances the corrosion rate of the base metal by improving the transport of the mass of the dissolved oxygen to the metal surface [33].

3.5.2. SEM and EDS analyses after 100% humidity test

Figs. 7a to 7b show the amorphous, dough-like morphology of corrosion products which are consistent with the earlier studies [22]. Corrosion products (Fig. 7b) offer a voluminous, spongy pompom-like appearance with granular morphology formed due to relative humidity and its interaction with the oxygen in the air, which might be $Zn_5(OH)_6(CO_3)_2$ [7,20,22,29]. The galvanised surface absorbs moisture and thereby leads to higher corrosion.

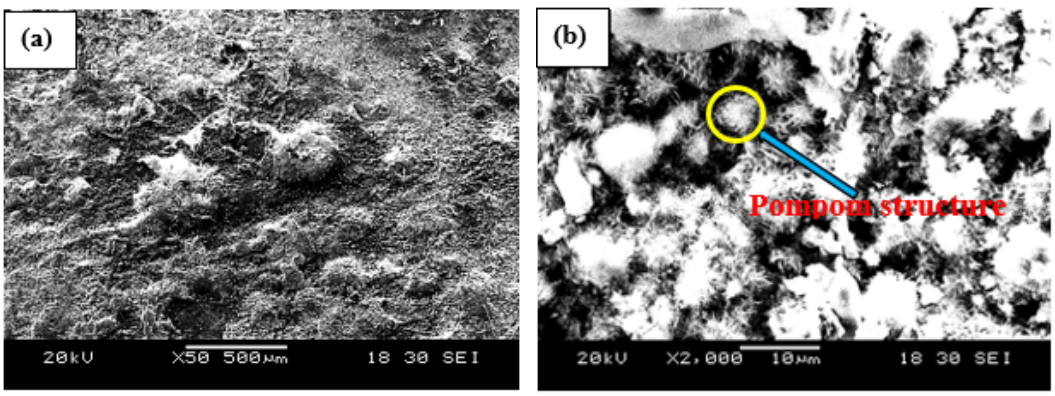

Fig. 7. SEM micrographs of the corroded galvanised sample after 100% humidity test at (a) 50× magnification and (b) 2000× magnification

A higher corrosion behaviour of galvanised steel sample in higher humidity has been reported earlier [7,38-39]. At higher relative humidity, the thickness of adsorbed water layer is more than ten monolayers and behaves like a bulk solution; thereby providing a hydration medium and enhancing the mobilization of ions [39].

3.5.3. SEM and EDS analyses after cyclic voltammetry

Figs. 8a to c depict the SEM images of the corroded galvanised, galvalume and colour-coated samples, respectively, after the cyclic voltammetry. For galvanised sample (Fig. 8a), different agglomerates of circular white granules were formed on the zinc coating in a localised manner. The sample surface shows the appearance of loose corrosion products. Fig. 8b shows the small islands with layered structures of rosette shapes formed due to local agglomerates of chlorides and moisture. This structure has occurred due to the presence of simonkolleite [9,46]. During corrosion, amorphous $Zn(OH)_2$ forms on the surface of the coating, which transforms to β-$Zn(OH)_2$ and dehydrates to ZnO finally, whereas simonkolleite forms in chloride solution, which protects the sample surface by forming a passive layer of Zn [9,18]. The peeling of the coating usually occurs at the interface of the metal coating/paint. It is because the conversion coating composition varies throughout the coating thickness, so closer metallic surfaces become enhanced in oxides/hydroxides of metals while that away from the surface contains compounds from the treated chemicals. These compositional differences in conversion coating influence their property too. These conversion coatings are not well adherent to the galvanised steel surface, which weakens the substrate/paint interface due to varying electrical conductivities of oxides and their salts. Inhibition of clustering and compaction of corrosion products were seen for the zinc oxide and its salts due to relatively higher conductivity. On the other hand, the non-conducting nature of aluminium oxides and their salts allows them to cluster easily. The properties of the conversion coatings affect the adhesive properties of the substrate top to a greater extent. Due to the above reasons, relatively low adhesion for paints was seen for zinc-rich galvanised steel coatings, while the Al-rich galvalume sample coatings and polyurethane-coated colour-coated samples show good adhesion and enhanced corrosion resistance. Better properties of polyurethane coating were reported earlier [1,16]. However, Mobin et al. have reported the poor behaviour of polyurethane coating due to coating detachment, but in the present study, this coating gives enhanced performance due to strong adhesion between the metal and coating [13].

Figs. 9 to 11 represent the micrographs of SEM and their corresponding EDS analyses of the corroded galvanised, galvalume and colour-coated sample surface, respectively. A deterioration in the sample surface smoothness reveals the chloride ion penetration that leads to the formation of the corrosion product, which was evident from the SEM micrographs. However, the extent of corrosion damage for colour-coated specimens is significantly less. EDS analysis reveals the chemical composition of the corrosion product. As all the experimental samples have low carbon steel substrates with different coatings, the expected

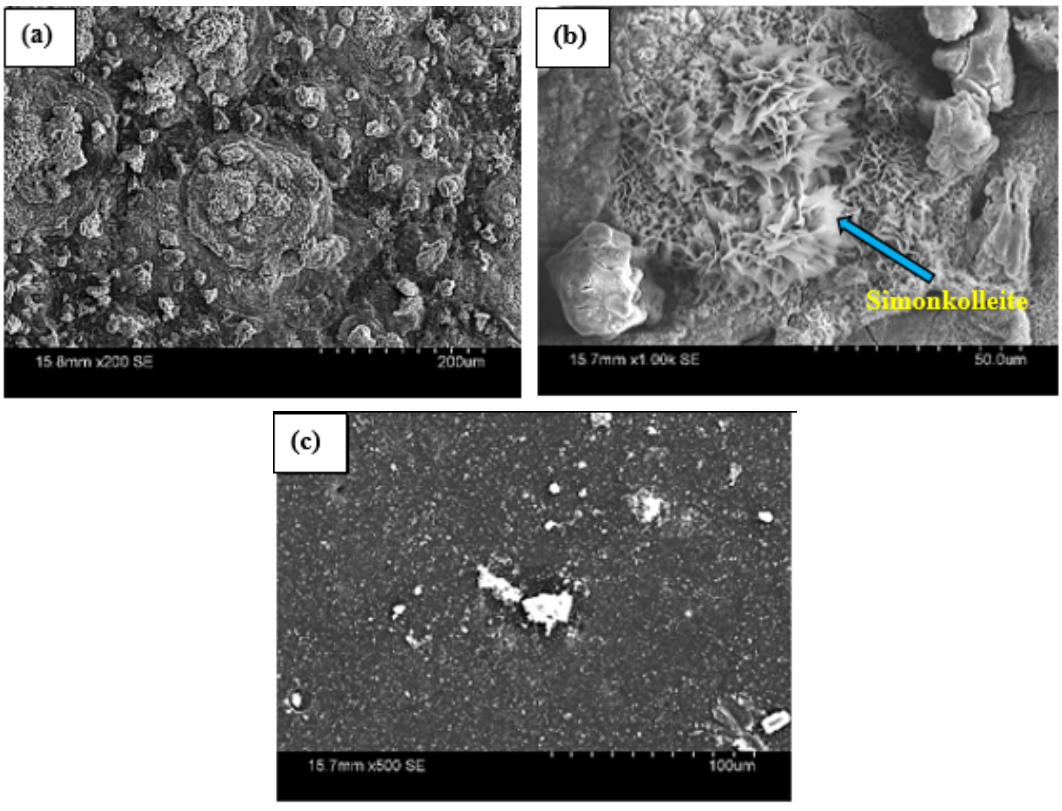

Fig. 8. SEM images after cyclic voltammetry for (a) galvanised, (b) galvalume and (c) colour-coated steel samples

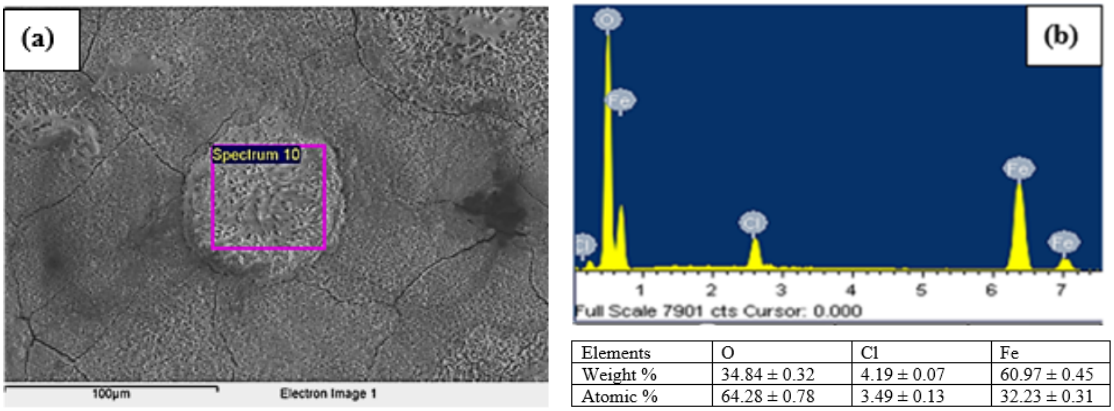

Elements	O	Cl	Fe
Weight %	34.84 ± 0.32	4.19 ± 0.07	60.97 ± 0.45
Atomic %	64.28 ± 0.78	3.49 ± 0.13	32.23 ± 0.31

Fig. 9. SEM image showing (a) corroded sample surface of the galvanised specimen and (b) EDS analysis from the denoted region of (a)

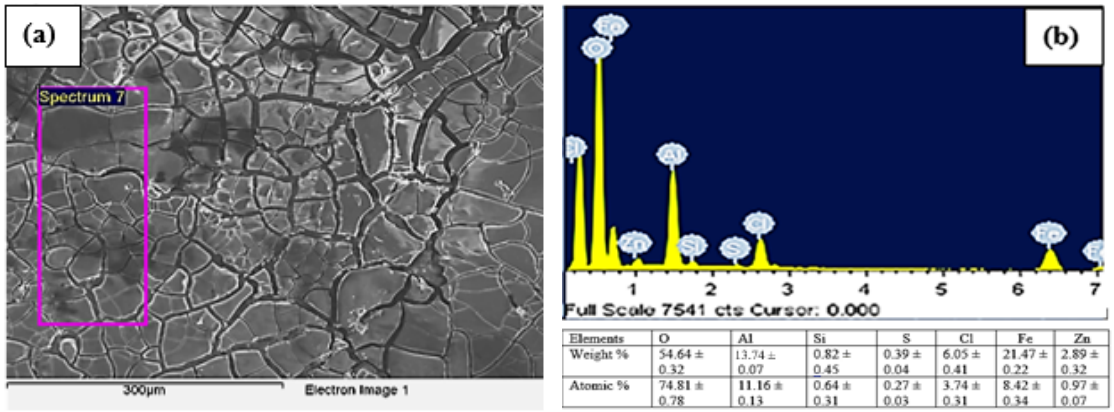

Elements	O	Al	Si	S	Cl	Fe	Zn
Weight %	54.64 ± 0.32	13.74 ± 0.07	0.82 ± 0.45	0.39 ± 0.04	6.05 ± 0.41	21.47 ± 0.22	2.89 ± 0.32
Atomic %	74.81 ± 0.78	11.16 ± 0.13	0.64 ± 0.31	0.27 ± 0.03	3.74 ± 0.31	8.42 ± 0.34	0.97 ± 0.07

Fig. 10. SEM image showing (a) corroded sample surface of galvalume specimen and (b) EDS analysis from the denoted region of (a)

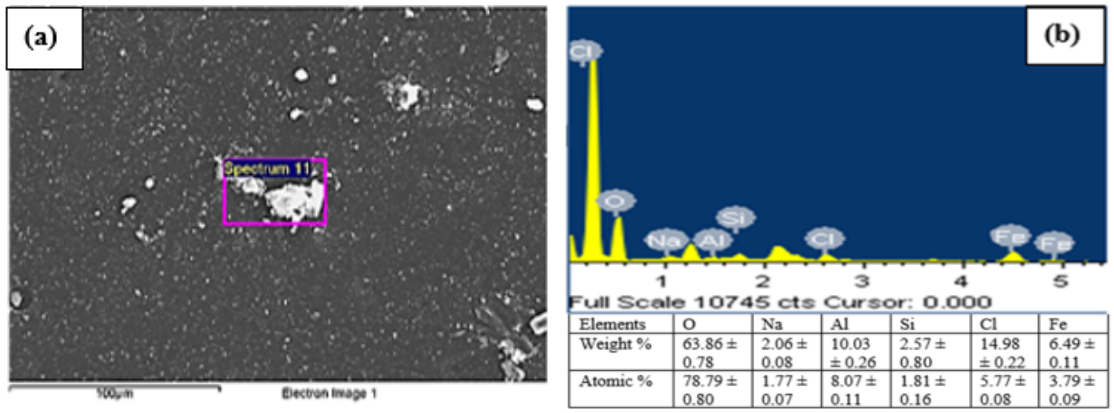

Elements	O	Na	Al	Si	Cl	Fe
Weight %	63.86 ± 0.78	2.06 ± 0.08	10.03 ± 0.26	2.57 ± 0.80	14.98 ± 0.22	6.49 ± 0.11
Atomic %	78.79 ± 0.80	1.77 ± 0.07	8.07 ± 0.11	1.81 ± 0.16	5.77 ± 0.08	3.79 ± 0.09

Fig. 11. SEM image showing (a) corroded surface of the colour-coated specimen and (b) EDS analysis from the denoted region of (a)

corrosion products are oxides, hydroxides and oxychlorides of Fe and Zn. The appearance of Fe and Cl in the spectrum (Fig. 9b) depicts the damage of the zinc coating under the influence of Cl^- ions. Furthermore, a higher amount of oxygen depicts higher corrosion [25]. Fig. 10a shows micro-meter sized corrosion products. Furthermore, cracks and spherical voids are formed in the galvalume coating. The higher amount of O, Fe, and Cl, as evident from the spectrum (Fig. 10b), depicts the corrosion of the galvalume specimen. In general, the lower corrosion rate of galvalume steel is attributed to the lesser Zn release rate compared to that of the galvanised sample due to the formation of an Al-rich phase (Al_2O_3) that acts as a barrier [47]. Micro galvanic effects between the active zinc-rich phase and passive aluminium-rich phase trigger the initial corrosion, which leads to the creation of a local corrosion cell [18]. Furthermore, chloride deposits over the sample surface led to damage in the passive layer of Al_2O_3 to start corrosion. Figs. 11a and 11b show the SEM image of the corroded colour-coated sample with the corresponding EDS analysis. The coating appears almost intact from corrosion except for a few locations on which EDS analysis is performed. A higher amount of O, Cl and Na found from the corroded region (denoted in Fig. 11a) indicates higher

corrosion. It is noteworthy that due to better adhesion and higher flexibility of polyurethane over the galvanised metal substrate, higher corrosion resistance is well accepted for the colour-coated sample. The better corrosion resistance of polyurethane coating is well-known and reported earlier [1,13].

3.6. Correlation between corrosion and its mechanism

Fig. 12 shows the schematics of the white and red rust formation for galvanised steel. Fig. 12a shows the uncorroded sample, whereas Fig. 12b shows the ingress of the chloride ions from NaCl and oxygen ions from the atmosphere into the zinc coating, which results in the formation of the anodic region which releases Zn^{2+} ions and 2 electrons; these 2 electrons from anode moves to the cathode and a cathodic reaction of OH^- formation occurs; thereby leads to the formation of a galvanic cell which undergoes through the galvanic corrosion. According to Cachet et al. [48], zinc dissolution in an aqueous solution depends on the adsorbed intermediate species (Zn_{ad}^{+}, Zn_{ad}^{2+} and $ZnOH_{ad}$) as follows:

$$Zn \rightleftarrows Zn_{ad}^{+} + e^{-} \quad (1)$$

$$Zn_{ad}^{+} \rightarrow e^{-} + Zn_{ad}^{2+} \quad (2)$$

$$Zn + H_2O \rightarrow \frac{1}{2}H_2 + ZnOH_{ad} \quad (3)$$

Therefore, a self-catalytic role is played by the intermediate species adsorbed on the surface of the electrode in the corrosion of zinc coating:

$$Zn_{ad}^{+} + Zn \rightarrow Zn_{sol}^{2+} + Zn_{ad}^{+} + 2e^{-} \quad (4)$$

$$Zn_{ad}^{2+} \rightarrow Zn^{2+} \quad (5)$$

$$ZnOH_{ad} + Zn \rightarrow ZnOH_{ad} + Zn_{sol}^{2+} + 2e^{-} \quad (6)$$

$$ZnOH_{ad} \rightarrow ZnOH_{sol}^{+} + e^{-} \quad (7)$$

$$ZnOH_{sol}^{+} \rightarrow Zn_{sol}^{2+} + OH^{-} \quad (8)$$

The onset of the zinc coating corrosion begins with the zinc dissolution at areas of the anode in an aqueous solution, which depends on three intermediates corresponding to the reaction ((1)-(8)). An oxygen reduction reaction in cathodic areas balances the anodic oxidation (9) in an alkaline medium [6].

$$O_2 + 2H_2O + 4e^{-} \rightarrow 4OH^{-} \quad (9)$$

The generation of initial rust layers results from the reaction of OH^- and Zn^{2+} ions. The overall reaction is given by equation (10).

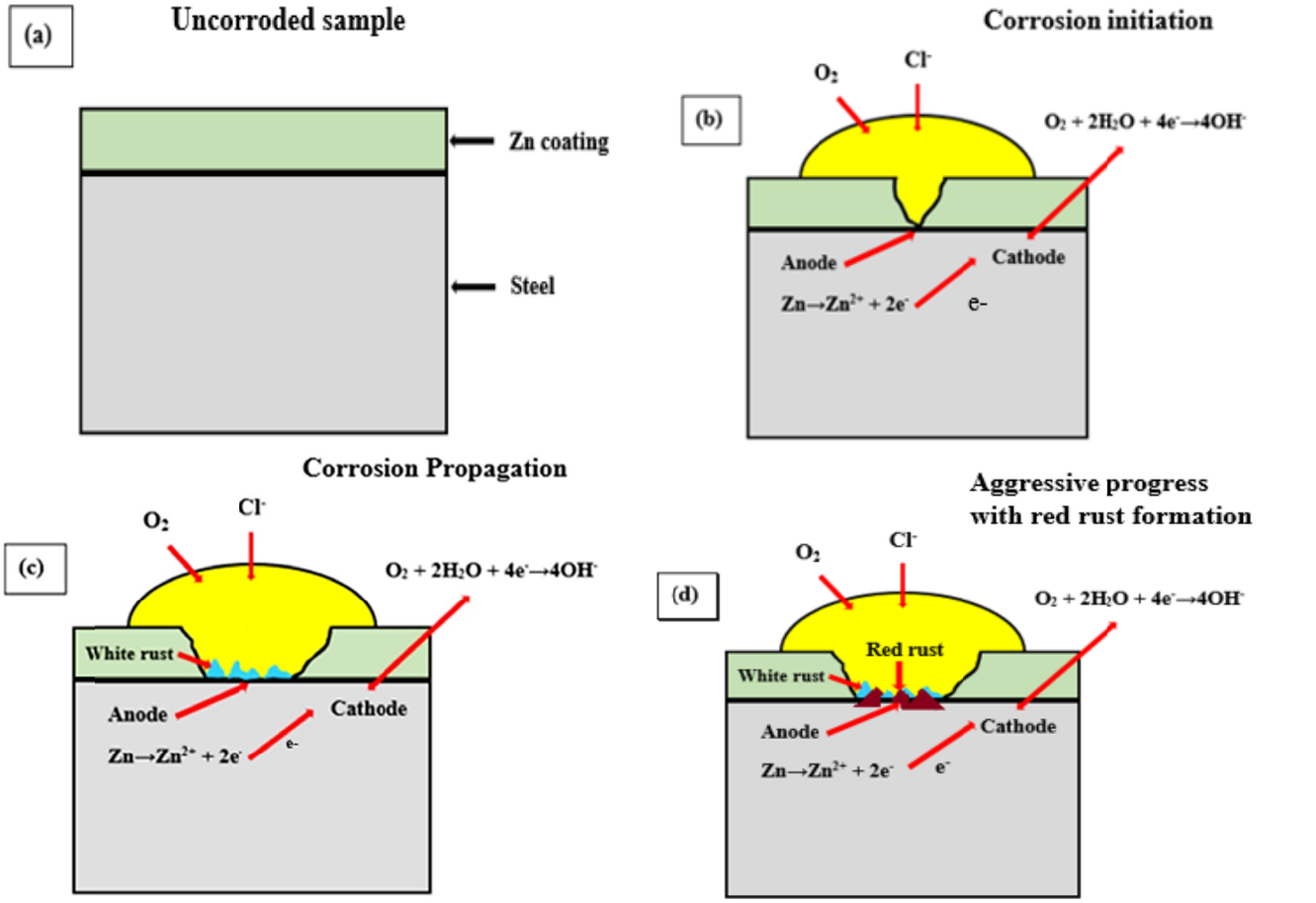

Fig. 12. Schematic illustration of the (a) uncorroded sample, (b) corrosion initiation, (c) corrosion propagation and (d) aggressive progress with red rust formation in the galvanised sample

$$2Zn(s) + O_2 + \\ + 2H_2O \rightarrow 2Zn(OH)_2 \rightleftarrows 2ZnO + 2H_2O \quad (10)$$

ZnO is considered as a semiconductor with low electrical conductivity; thereby enhancing the resistance to corrosion of zinc coating [6]. It is a well-known fact that Cl^- is an anode activator which induces pitting corrosion, and the cyclic voltammetry and SEM study of salt spray samples confirms this fact [6,32,49]. In the presence of NaCl, Cl^- migrates to the anodic sites and forms $Zn_5(OH)_8Cl_2$ according to equation (11) [6,50-51]:

$$5ZnO + 2Cl^- + \\ + 6H_2O \rightarrow Zn_5(OH)_8Cl_2.H_2O(s) + 2OH^- \quad (11)$$

$Zn_5(OH)_8Cl_2.H_20$ is known as simonkolleite which is confirmed from XRD, mainly leads to the formation of white rust, which has corrosion resistance properties as discussed in earlier sections, and it tries to prevent corrosion of the sample as seen from Fig. 12c, but due to its thermodynamic instability as well as its localised nature to form the corrosion products, it usually fails to cover the entire area of the metal surface to prevent the corrosion of the sample and Cl^- ions continue to enter through the local breaks in the areas where these simonkolleite are absent and thereby reaches the base metal of iron, and once it does that, it then starts to corrode the base metal with the following reactions (i.e., equations (12)-(17)) [52].

Anodic reactions:

$$Fe \rightarrow Fe^{2+} + 2e^- \quad (12)$$

$$Fe^{2+} \rightarrow Fe^{3+} + e^- \quad (13)$$

Total reaction:

$$Fe^{2+} + 2OH^- \rightarrow Fe(OH)_2 \quad (14)$$

$$2Fe(OH)_2 + Cl^- \rightarrow Fe_2(OH)_3Cl + OH^- + e^- \quad (15)$$

$$Fe_2(OH)_3Cl + \\ + 2H_2O \rightarrow Fe_4(OH)_8Cl + e^- + 2H^+ + Cl^- \quad (16)$$

$$Fe_4(OH)_8Cl(\textit{via oxidation}) \rightarrow \beta - FeOOH \quad (17)$$

The formation of akagainite through various reactions is given from equations (14)-(17). The oxidation of Fe to give Fe^{2+} under the influence of corrosion, which reacts with OH^- ions to form Iron hydroxide, that under the influence of Cl^- gives $Fe_2(OH)_3Cl$, which further reacts with water to form green rust ($Fe_4(OH)_8Cl$) and this finally oxidised to give β-FeOOH (akagainite) which enhances corrosion rate [53-54]. It is well known that β-FeOOH is usually found in high chloride environments, which enhances corrosion [52-54]. This compound is found in the thick parts of the rust layers and rarely found in thin parts and works as a reservoir of chloride ions and this enhances the porosity of the rust to allow the entry of chloride ions from outside easily to promote corrosion [52]. Due to this corrosion of the base metal of iron, red rust starts to appear on the metal surface which is a mixture of β-FeOOH, Fe_3O_4, FeOH, Fe_2O_3, δ-FeOH and corrosion starts to progress more aggressively and thereby, metal starts to corrode at a faster rate as evident in Fig. 12d.

4. Conclusions

The major conclusions obtained from the current study are given below:

(1) Various corrosion tests like salt spray test, 100% relative humidity test and chemical resistance test were performed. The salt spray test reveals white and red rusts for galvanised samples, while galvalume and colour-coated samples remain intact from corrosion, whereas the 100% relative humidity test and chemical resistance test show higher corrosion for galvanised sample. So, corrosion resistance of samples in atmospheric conditions as well as in salty environments, rainy environments and resistance to household chemicals follows the trend as colour-coated steel > galvalume > galvanised.

(2) Cyclic voltammetry and linear polarization studies were performed to study the pitting corrosion and marine environmental corrosion behaviour. Cyclic voltammetry reveals slightly higher pitting corrosion for the galvalume sample than the other two steels due to the acidic nature of the solution which accelerates the corrosion process and also, coatings have weak barrier properties in these solutions. The higher corrosion resistance of colour-coated steel is attributed to a polyurethane coating.

(3) SEM and EDS analyses for the salt spray and 100% humidity-tested galvanised samples show various types of corrosion products with their morphologies. The presence of voids, loose corrosion products and flakes for the salt spray tested sample and voluminous, spongy pompom-like appearance with granular morphology formed in 100% relative humidity test are well documented and a comparative study of all three corroded samples after cyclic voltammetry study is also performed.

(4) XRD reveals the corrosion products in salt spray and 100% humidity tests for galvanised steel sample. For the salt spray tested sample, the X-ray profile primarily reveals $Zn_5(OH)_8Cl_2H_2O$ (simonkolleite), ZnO (zinc oxide), β-Zn $(OH)_2$, Zn $(OH)_2$ (zinc hydroxide) and Zn $(ClO_4)_2$ whereas for the 100% relative humidity tested sample, main corrosion products are ZnO (zinc oxide), β-Zn $(OH)_2$, Zn $(OH)_2$ (zinc hydroxide), Fe and Zn.

(5) Raman spectroscopy shows the spectacular result for salt spray and 100% humidity-tested corroded samples. For salt spray testing, ZnO, β-FeOOH, white rust, green rust, $FeCl_2$, Fe_3O_4, FeOH, Fe_2O_3 and δ-FeOH are present. But for 100% humidity corroded sample, only ZnO is present.

REFERENCES

[1] N. Arianpouya, M. Shishesaz, M. Arianpouya, M. Nematollahi, Evaluation of synergistic effect of nanozinc/nanoclay additives on the corrosion performance of zinc-rich polyurethane nanocomposite coatings using electrochemical properties and salt spray testing. Surf. Coat. Technol. **216**, 199-206 (2013). DOI: https://doi.org/10.1016/j.surfcoat.2012.11.036

[2] T.A. Kepperta, G. Luckenederb, K.H. Stellnbergerb, G. Moria, H. Antrekowitsch, Investigation of the corrosion behavior of Zn-Al-Mg hot-dip galvanised steel in alternating climate tests. Corrosion **70** (12), 1238-1248 (2014). DOI: https://doi.org/10.5006/1158

[3] B. Boelen, B. Schimitz, J. Defourny, F. Blekkenhorst, A literature survey on the development of an accelerated laboratory test method for atmospheric corrosion of precoated steel products. Corros. Sci. **34** (11), 1923-1931 (1993). DOI: https://doi.org/10.1016/0010-938X(93)90028-F

[4] S. Schürz, G.H. Luckeneder, M. Fleischanderl, P. Mack, H. Gsaller, A.C. Kneissl, G. Mori, Chemistry of corrosion products on Zn–Al–Mg alloy coated steel. Corros. Sci. **52** (10), 3271-3279 (2010). DOI: https://doi.org/10.1016/j.corsci.2010.05.044

[5] A.K. Singh, G. Jha, N. Rani, N. Bandyopadhyay, T. Venugopalan, Premature darkening problem and its prevention in galvanised sheet surface. Surf. Coat. Technol. **200** (16-17), 4897-4903 (2006). DOI: https://doi.org/10.1016/j.surfcoat.2005.04.044

[6] H. Sun, S. Liu, L. Sun, A comparative study on the corrosion of galvanised steel under simulated rust layer solution with and without 3.5wt%NaCl. Int. J. Electrochem. Sci. **8**, 3494-3509 (2013).

[7] E.D. Angel, R. Vera, F. Corvo, Atmospheric corrosion of galvanised steel in different environments in Chile and Mexico. Int. J. Electrochem. Sci. **10**, 7985-8004 (2015).

[8] L. Kwiatkowski, J. Kwiecied, T. Szustkiewicz, Accelerated corrosion tests for protective properties for aluminium and zinc coatings. Mater. Sci. **32**, 681-687 (1996). DOI: https://doi.org/10.1007/BF02538570

[9] A.P.D. Santos, S.M. Manhabosco, J.S. Rodrigues, L.F.P. Dick, Comparative study of the corrosion behaviour of galvanised, galvannealed and Zn55Al coated interstitial free steels. Surf. Coat. Technol. **279**, 150-160 (2015). DOI: https://doi.org/10.1016/j.surfcoat.2015.08.046

[10] F. Deflorian, S. Rossi, M. Fedel, Organic coating degradation: comparison between natural and artificial weathering. Corros. Sci. **50** (8), 2360-2366 (2008). DOI: https://doi.org/10.1016/j.corsci.2008.06.009

[11] S. Schuerz, M. Fleischanderl, G.H. Luckeneder, K. Preis, T. Haunschmied, G. Mori, A.C. Kneissl, Corrosion behaviour of Zn–Al–Mg coated steel sheet in sodium chloride-containing environment. Corros. Sci. **51** (10), 2355-2363 (2009). DOI: https://doi.org/10.1016/j.corsci.2009.06.019

[12] X. Zhang, T.N. Vu, P. Volovitch, C. Leygraf, K. Ogle, I.O. Wallinder, The initial release of zinc and aluminium from non-treated galvalume and the formation of corrosion products in chloride containing media. Appl. Surf. Sci. **258** (10), 4351-4359 (2012). DOI: https://doi.org/10.1016/j.apsusc.2011.12.112

[13] M. Mobin, A.U. Malik, F. Al-Muaili, M. Al-Hajri, Performance evaluation of a commercial polyurethane coating in marine environment. J. Mater. Eng. Perform. **21**, 1292-1299 (2012). DOI: https://doi.org/10.1007/s11665-011-0034-x

[14] M. Hattori, A. Nishikata, T. Tsuru, EIS study on degradation of polymer coated steel under ultraviolet radiation. Corros. Sci. **52** (6), 2080-2087 (2010). DOI: https://doi.org/10.1016/j.corsci.2010.01.038

[15] A.R. Marder, The metallurgy of zinc-coated steel. Prog. Mater. Sci. **45** (3), 191-271 (2000). DOI: https://doi.org/10.1016/S0079-6425(98)00006-1

[16] R.P. Edavan, R. Kopinski, Corrosion resistance of painted zinc alloy coated steels. Corros. Sci. **51** (10), 2429-2442 (2009). DOI: https://doi.org/10.1016/j.corsci.2009.06.028

[17] J.G. Speight, Section-1: inorganic chemistry, Table 1.71, Lange's Handbook of Chemistry, 2005 McGraw Hill, New York.

[18] X. Zhang, I.O. Wallinder, C. Leygraf, Atmospheric corrosion of Zn–Al coatings in a simulated automotive environment. Surf. Eng. **34** (9), 641-648 (2017). DOI: https://doi.org/10.1080/02670844.2017.1305658

[19] M. Manna, M. Dutta, A.N. Bhagat, Microstructure and electrochemical performance evaluation of Zn, Zn-5 wt.% Al and Zn-20 wt.% Al alloy coated steels. J. Mater. Eng. Perform. **30** (1), 627-637 (2021). DOI: https://doi.org/10.1007/s11665-020-05359-8

[20] C. Li, R. Ma, A. Du, Y. Fan, X. Zhao, X. Cao, Superhydrophobic film on hot-dip galvanised steel with corrosion resistance and self-cleaning properties. Metals **8** (9), 1-17 (2018). DOI: https://doi.org/10.3390/met8090687

[21] A.S. Sergienko, G.V. Redkin, A.S. Rozhkov, Y.I. Kuznetsov, Corrosion inhibition of galvanised steel by thin superhydrophobic phosphonate–siloxane films. Int. J. Corros. Scale Inhib. **11** (1), 322-338 (2022). DOI: https://doi.org/10.17675/2305-6894-2022-11-1-19

[22] D. Persson, D. Thierry, O. Karlsson, Corrosion and corrosion products of hot dipped galvanised steel during long term atmospheric exposure at different sites world-wide. Corros. Sci. **126**, 152-165 (2017). DOI: https://doi.org/10.1016/j.corsci.2017.06.025

[23] T.C. Simpson, Accelerated corrosion test for aluminium-zinc alloy coatings. Corrosion **49** (7), 550-560 (1993). DOI: https://doi.org/10.5006/1.3316084

[24] S.P. Ali, C. Dehghanian, A. Kosari, Corrosion protection of the reinforcing steels in chloride-laden concrete environment through epoxy/polyaniline-camphorsulfonate nanocomposite coating. Corros. Sci. **90**, 239-247 (2015). DOI: https://doi.org/10.1016/j.corsci.2014.10.015

[25] M. Yadav, I. Dey, S.K. Ghosh, A comparative study on the microstructure, hardness and corrosion resistance of epoxy coated and plain rebars. Mater. Res. Express. **9**, 055504 (2022). DOI: https://doi.org/10.1088/2053-1591/ac6857

[26] A. Macias, C. Andrade, Corrosion of galvanised steel reinforcements in alkaline solution. Part I: Electrochemical results. Brit. Corros. J. **22** (2), 113-118 (1987). DOI: https://doi.org/10.1179/000705987798271631

[27] F. Altmayer, Critical aspects of the salt spray test. Plating Surf. Finish. (1985).

[28] L. Dosdat, J. Petitjean, T. Vietoris, O. Clauzeau, Corrosion resistance of different metallic coatings on press-hardened steels for automotive. Steel Res. Int. **82** (6), 726-735 (2011). DOI: https://doi.org/10.1002/srin.201000291

[29] M. Zapponi, T. Pérez, C. Ramos, C. Saragovi, Prohesion and outdoors tests on corrosion products developed over painted galvanised steel sheets with and without Cr (VI) species. Corros. Sci. **47** (4), 923-936 (2005). DOI: https://doi.org/10.1016/j.corsci.2004.06.007

[30] Y. Liu, H. Li, Z. Li, EIS investigation and structural characterisation of different hot-dipped zinc-based coatings in 3.5%NaCl solution. Int. J. Electrochem. Sci. **8**, 7753-7767 (2013).

[31] E. Palma, J. M. Puente, M. Morcillo, The atmospheric corrosion mechanism of 55%Al-Zn coating on steel. Corros. Sci. **40** (1), 61-68 (1998). DOI: https://doi.org/10.1016/S0010-938X(97)00112-1

[32] E. Dubuisson, P. Lavie, F. Dalard, J.P. Caire, S. Szunerits, Corrosion of galvanised steel under an electrolytic drop. Corros. Sci. **49** (2), 910-919 (2007). DOI: https://doi.org/10.1016/j.corsci.2006.05.027

[33] V.B. Moreira, A. Krummenauer, J.Z. Ferreira, H.M. Veit, E. Armelin, A. Meneguzzi, Computational image analysis as an alternate tool for the evaluation of corrosion in salt spray test. Stud. Ubb Chem. **65** (3), 45-61 (2020). DOI: https://doi.org/10.24193/subbchem.2020.3.04

[34] J.K. Odusote, O.S. Ayanda, Y.R. Abolore, Inhibition of corrosion of galvanised steel sheet in 1M HCl and H_2SO_4 by plukenetia conophora leaf extract. African Corros. J. 14-18 (2016).

[35] G. Vourlias, N. Pistofidis, G. Stergioudis, E. Pavlidou, D. Tsipas, Influence of alloying elements on the structure and corrosion resistance of galvanised coatings. Phys. Stat. Sol. A. **201** (7), 1518-1527 (2004). DOI: https://doi.org/10.1002/pssa.200306799

[36] R. Autengruber, G. Luckeneder, A.W. Hassel, Corrosion of press-hardened galvanised steel. Corros. Sci., **63**, 12-19 (2012). DOI: https://doi.org/10.1016/j.corsci.2012.04.048

[37] G.A. El-Mahdy, A. Nishikata, T. Tsuru, Electrochemical corrosion monitoring of galvanised steel under cyclic wet-dry conditions. Corros. Sci. **42** (1), 183-194 (2000). DOI: https://doi.org/10.1016/S0010-938X(99)00057-8

[38] K. Suzumura, S. Nakamura, Environmental factors affecting corrosion of galvanised steel wires. J. Mater. Civil Eng. **16**, 1-7 (2004). DOI: https://doi.org/10.1061/(ASCE)0899-1561(2004)16:1(1)

[39] S.C. Chung, S.L. Sung, C.C. Hsien, H.C. Shih, Application of EIS to the initial stages of atmospheric zinc corrosion. J. Appl. Electrochem. **30**, 607-615 (2000). DOI: https://doi.org/10.1023/A:1003908219469

[40] E. Diler, B. Rouvellou, S. Rioual, B. Lescop, G.N. Vien, D. Thierry, Characterisation of corrosion products of Zn and Zn–Mg–Al coated steel in a marine atmosphere. Corros. Sci. **87**, 111-117 (2014). DOI: https://doi.org/10.1016/j.corsci.2014.06.017

[41] K. Tano, S. Higuchi, Development and properties of zinc-aluminium alloy coated steel sheet with high corrosion resistance (super zinc). Nippon Steel Tech. Rep. **25**, 29-37 (1985).

[42] Z.I. Ortiz, P. Díaz-Arista, Y. Meas, R. Ortega-Borges, G. Trejo, Characterization of the corrosion products of electrodeposited Zn, Zn–Co and Zn–Mn alloys coatings. Corros. Sci. **51** (11), 2703-2715 (2009). DOI: https://doi.org/10.1016/j.corsci.2009.07.002

[43] H.H. Hassan, Corrosion behaviour of zinc in sodium perchlorate solutions. Appl. Surf. Sci. **174** (3-4), 201-209 (2001). DOI: https://doi.org/10.1016/S0169-4332(01)00154-4

[44] Ph. Colomban, S. Cherifi, G. Despert, Raman identification of corrosion products on automotive galvanised steel sheets. J. Raman Spectrosc. **39** (7), 881-886 (2008). DOI: https://doi.org/10.1002/jrs.1927

[45] W. Miao, I.S. Cole, A.K. Neufeld, S. Furman, Pitting corrosion of Zn and Zn-Al coated steels in pH 2 to 12 NaCl solution. J. Electrochem. Soc. **154** (1) C7 (2007).

[46] W. Xu, L. Wei, Z. Zhang, Y. Liu, K.C. Chou, H. Fan, Q. Li, Effects of lanthanum addition on the microstructure and corrosion resistance of galvanised coating. J. Alloys Compd. **784**, 859-868 (2019). DOI: https://doi.org/10.1016/j.jallcom.2019.01.075

[47] P. Qiu, C. Leygraf, I.O. Wallinder, Evolution of corrosion products and metal release from galvalume coatings on steel during short and long-term atmospheric exposures. Mater. Chem. Phys. **133** (1), 419-428 (2012). DOI: https://doi.org/10.1016/j.matchemphys.2012.01.054

[48] C. Cachet, F. Ganne, G. Maurin, J. Petitjean, V. Vivier, R. Wiart, EIS investigation of zinc dissolution in aerated sulfate medium. Part I: bulk zinc. Electrochim. Acta. **47** (3), 509-518 (2001). DOI: https://doi.org/10.1016/S0013-4686(01)00740-X

[49] H. Zhang, X.G. Li, C.W. Du, H.B. Qi, Corrosion behaviour and mechanism of the automotive hot dip galvanised steel with alkaline mud adhesion. Int. J. Miner. Metall. Mater. **16** (4), 414-421 (2009). DOI: https://doi.org/10.1016/S1674-4799(09)60073-X

[50] Q. Qu, C. Yan, Y. Wan, C. Cao, Effects of NaCl and SO_2 on the initial atmospheric corrosion of zinc. Corros. Sci. **44** (12), 2789-2803 (2002). DOI: https://doi.org/10.1016/S0010-938X(02)00076-8

[51] Y. Li, Formation of nano-crystalline corrosion products on Zn–Al alloy coating exposed to seawater. Corros. Sci. **43** (9), 1793-1800 (2001). DOI: https://doi.org/10.1016/S0010-938X(00)00169-4

[52] Y. Ma, Y. Li, F. Wang, Corrosion of low carbon steel in atmospheric environments of different chloride contents. Corros. Sci. **51** (5), 997-1006 (2009). DOI: https://doi.org/10.1016/j.corsci.2009.02.009

[53] P. Refait, J.M.R. Genin, The mechanisms of oxidation of ferrous hydroxy chloride β-$Fe_2(OH)_3$ Clin aqueous solution: The formation of Akagainite vs Goethite. Corros. Sci. **39** (3), 539-553 (1997). DOI: https://doi.org/10.1016/S0010-938X(97)86102-1

[54] T. Misawa, T.W. Kyuno Suetaka, S. Shimodaira, The mechanism of atmospheric rusting and the effect of Cu and P on the rust formation of low alloy steels. Corros. Sci. **11** (1) 35-48 (1971). DOI: https://doi.org/10.1016/S0010-938X(71)80072-0